Nonlinear Optics (WiSe 2019/20)

Lecture 6: November 22, 2019

6 Acousto-optic modulators

6.1 Acousto-optic interaction

6.2 The acousto-optic amplitude modulator

Chapter 7: Third-order nonlinear effects

7.1 Third-harmonic generation (THG)

7.2 The nonlinear refractive index

7.3 Molecular orientation and refractive index

7.4 Self-phase modulation (SPM)

7.5 Self-focusing

6. Acousto-optic modulator
6.1 Acousto-optic interaction

In a linear acousto-optic medium, the refractive index change is proportional to the applied voltage, see Eq. (5.8). The wave equation is

$$\nabla \times \nabla \times \mathbf{E} = -\mu_0 \frac{\partial^2}{\partial t^2}\mathbf{D} = -\mu_0 \frac{\partial^2}{\partial t^2}\left(\varepsilon_0 \mathbf{E} + \mathbf{P}\right) \tag{6.1}$$

The time-varying displacement can be separated into a part described by a constant average susceptibility or refractive index n, and a time-varying contribution described by $\Delta n(r,t)$

$$\begin{aligned} \mathbf{D} &= \varepsilon_0 \mathbf{E} + \mathbf{P} = \varepsilon_0 \left(n + \Delta n(r,t)\right)^2 \mathbf{E} \\ &\approx \varepsilon_0 n^2 \mathbf{E} + 2\varepsilon_0 n \Delta n(r,t)\mathbf{E}, \end{aligned} \tag{6.2}$$

where we neglect potential higher-order terms in $\Delta n(r,t)$, i.e., $\Delta n(r,t) \ll n$. From Eqs. (6.1) and (6.2), we have

$$\nabla \times \nabla \times \mathbf{E} + \frac{1}{c^2}\frac{\partial^2 \mathbf{E}}{\partial t^2} = -2\frac{1}{c^2}\frac{\partial^2}{\partial t^2}\left[\frac{\Delta n(r,t)}{n}\mathbf{E}\right] \tag{6.3}$$

with $c^2 = 1/(\varepsilon_0 \mu_0 n^2)$. We consider a plane electromagnetic wave with wave vector $\mathbf{k}_i$ in the x-z-plane, see Fig. 6.1.

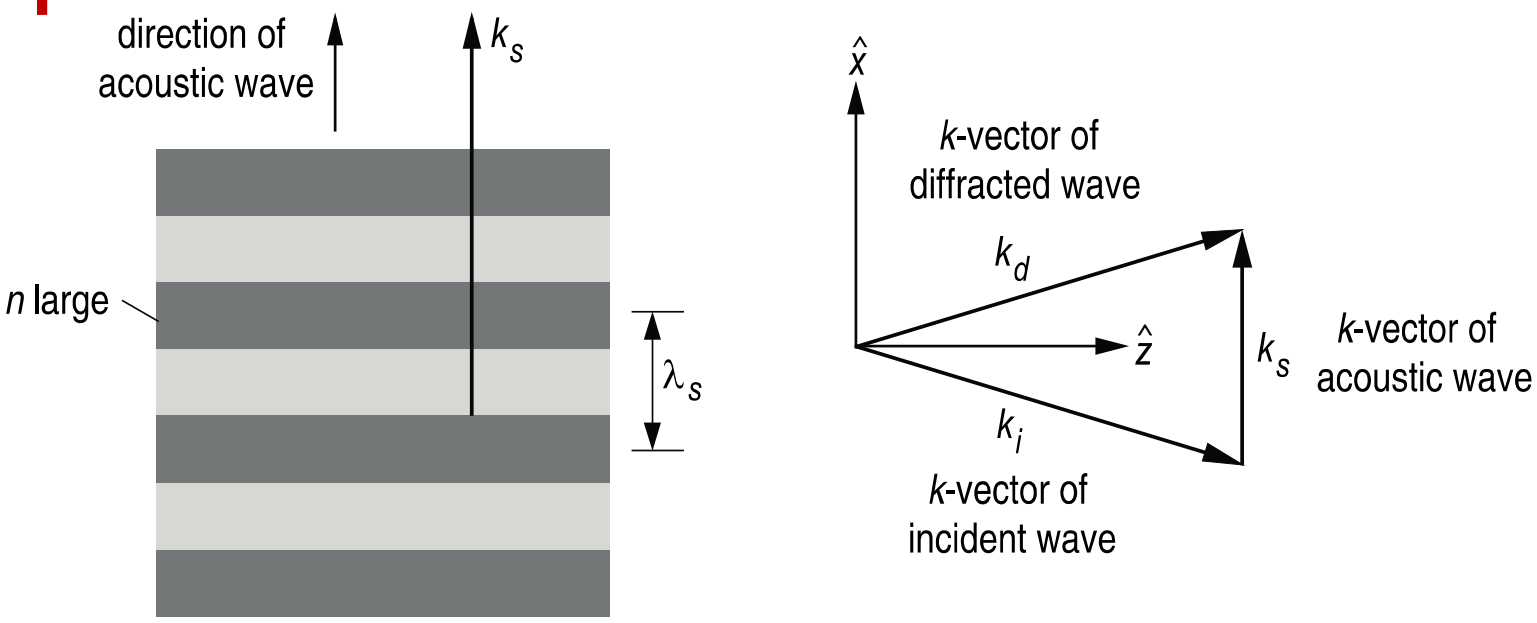

Figure 6.1: Diffraction grating in a medium generated by an acoustic wave.

The refractive index change generated by a wave with frequency ω_s is proportional to the acoustic wave

$$\begin{aligned}\Delta n(r,t) &= \Delta\hat{n}\cos\left(\omega_s t - \mathbf{k}_s\cdot\mathbf{r}\right)\\ &= \frac{\Delta\hat{n}}{2}\left[e^{j(\omega_s t-\mathbf{k}_s\cdot\mathbf{r})}+e^{-j(\omega_s t-\mathbf{k}_s\cdot\mathbf{r})}\right].\end{aligned} \tag{6.4}$$

$\Delta\hat{n}$ is the amplitude of the resulting refractive index wave. From Gauss law for the electric field

$$\nabla\cdot\varepsilon\mathbf{E} = \rho = \varepsilon\nabla\cdot\mathbf{E}+\mathbf{E}\cdot\nabla\varepsilon, \tag{6.5}$$

with

$$\varepsilon = \varepsilon_0\left(n+\Delta n(r,t)\right)^2 \approx \varepsilon_0\left(n^2+2n\Delta n(r,t)\right). \tag{6.6}$$

If the electric field is polarized along the y-direction, we obtain $\mathbf{E}\cdot\nabla\varepsilon = 0$. If there are in addition no charges ρ, then the divergence of $\mathbf{E}$ vanishes, and the wave equation (6.3) simplifies to

$$\boldsymbol{\Delta}\mathbf{E} - \frac{1}{c^2}\frac{\partial^2\mathbf{E}}{\partial t^2} = +2\frac{1}{c^2}\frac{\partial^2}{\partial t^2}\left[\frac{\Delta n(r,t)}{n}\mathbf{E}\right] \tag{6.7}$$

The time-dependent refractive index multiplies with the field, which initially consists of only an incident field with index i and a diffracted wave with index d is generated

$$\mathbf{E} = \hat{\mathbf{E}}_i e^{j(\omega_i t-\mathbf{k}_i\cdot\mathbf{r})} + \hat{\mathbf{E}}_d e^{j(\omega_d t-\mathbf{k}_d\cdot\mathbf{r})} + c.c. \tag{6.8}$$

The product of incoming wave and index modulation generates a polarization, which is the source for the diffracted wave. Therefore, there is

$$\omega_d = \pm\omega_s+\omega_i \quad \text{and} \quad \mathbf{k}_d = \pm\mathbf{k}_s+\mathbf{k}_i.$$

Usually, the frequency of sound is much less than the optical frequency, $\omega_s \ll \omega_i$, and therefore $|\mathbf{k}_d| \simeq |\mathbf{k}_i|$. Fig. 6.1 shows the resulting $\mathbf{k}$-diagram. We solve the wave equation (6.7) approximately, assuming that the amplitudes of the incoming and diffractive waves change slowly along the z-direction

$$\mathbf{E}_i = \mathbf{e}_y A_i(z) e^{j(\omega_i t - \mathbf{k}_i \cdot \mathbf{r})} + c.c. \tag{6.9}$$

$$\mathbf{E}_d = \mathbf{e}_y A_d(z) e^{j(\omega_d t - \mathbf{k}_d \cdot \mathbf{r})} + c.c. \tag{6.10}$$

If we substitute (6.7) into (6.8), and use the slowly varying envelope approximation (as in Chapter 3), we obtain

$$-\left(\mathbf{k}_d^2 - \frac{\omega_d^2}{c^2}\right) A_d(z) - 2j\mathbf{k}_d \cdot \nabla A_d(z) \simeq -\frac{\omega_d^2}{c^2} \Delta\hat{n} A_i(z) \tag{6.11}$$

$$-\left(\mathbf{k}_i^2 - \frac{\omega_i^2}{c^2}\right) A_i(z) - 2j\mathbf{k}_i \cdot \nabla A_i(z) \simeq -\frac{\omega_i^2}{c^2} \Delta\hat{n} A_d(z). \tag{6.12}$$

With $\mathbf{k}_{d,i}^2 = \frac{\omega_{d,i}^2}{c^2}$ and $\mathbf{k}_d \cdot \nabla A_d(z) = k_d \cos\theta \frac{dA_d}{dz}$, we obtain

$$\frac{dA_d(z)}{dz} \simeq -j\frac{\omega_d}{2c}\frac{\Delta\hat{n}}{\cos\theta} A_i(z) \tag{6.13}$$

$$\frac{dA_i(z)}{dz} \simeq -j\frac{\omega_i}{2c}\frac{\Delta\hat{n}}{\cos\theta} A_d(z). \tag{6.14}$$

This set of equations describes coupled modes. However, the coupling coefficients

$$\frac{\omega_d}{2c}\frac{\Delta\hat{n}}{\cos\theta} \text{ and } \frac{\omega_i}{2c}\frac{\Delta\hat{n}}{\cos\theta}$$

are not equal, because $\omega_d \neq \omega_i$. This results from the acoustic waves that excite and drive optical waves. However, the difference is small, on the order of a millionth. Therefore, we can neglect the difference in Eqs. (6.13) and (6.14) and obtain with the coupling coefficient

$$\kappa = \frac{\omega_d}{2c}\frac{\Delta\hat{n}}{\cos\theta} \simeq \frac{\omega_i}{2c}\frac{\Delta\hat{n}}{\cos\theta} \tag{6.15}$$

and initial conditions $A_d(z) = 0$ the solution

$$A_i(z) = A_i(0)\cos|\kappa|\, z \tag{6.16}$$

$$A_d(z) = -jA_i(0)\sin|\kappa|\, z. \tag{6.17}$$

The incoming wave is depleted along the propagation and transformed into a diffracted wave. The diffracted wave is slightly shifted in frequency. If the interaction length is long enough, so that $|\kappa|\, z > \pi/2$, the diffracted wave is

Applications:

Deflection of light

Frequency shifting

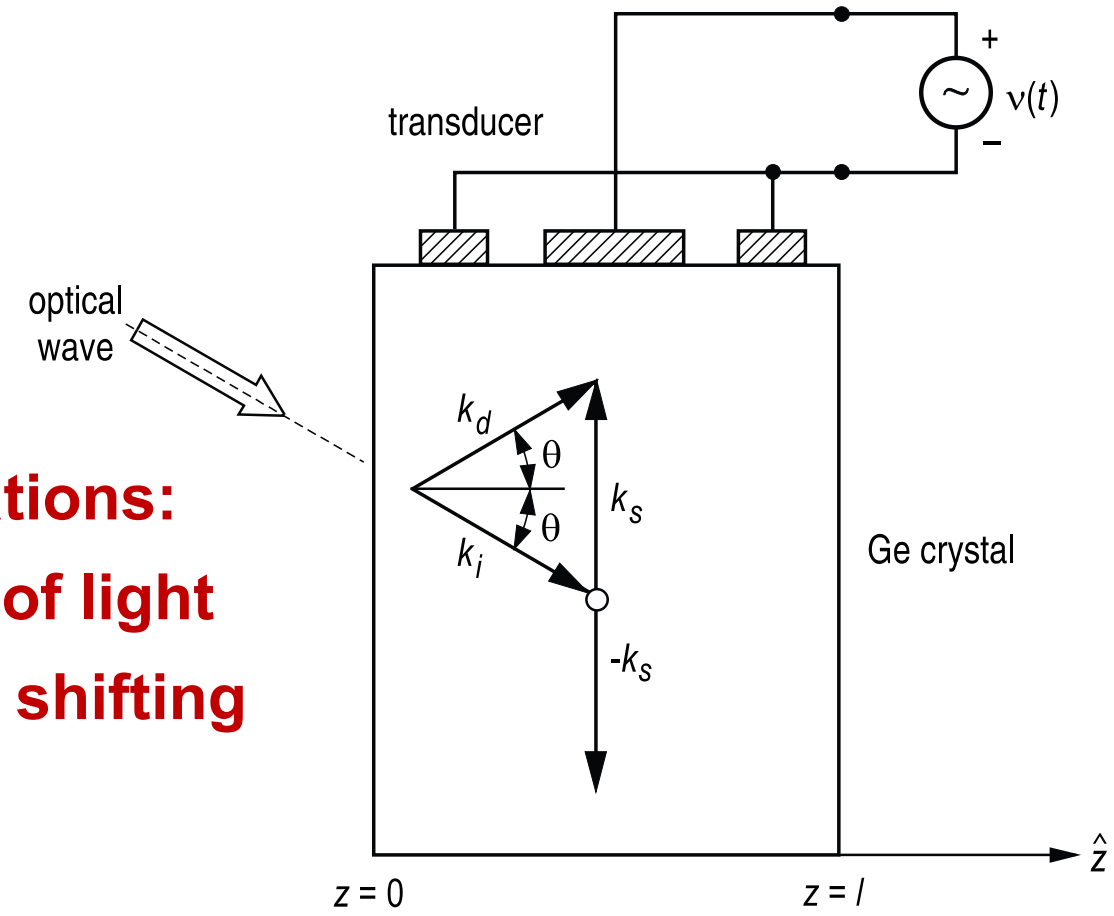

Figure 6.2: Typical **k**-diagram describing acousto-optic light diffraction at a standing acoustic wave.

Eqs. (6.16) and (6.17) also have a different meaning. If the frequency $\omega_s = 0$, then the optical wave interacts with a constant index grating. The diffracted wave has exactly the same frequency and the wave vectors must obey momentum conservation. Also this situation is described by the same coupled mode equations. The coupling coefficients are now identical and the total optical energy of both partial waves is conserved.

6.2 The acousto-optic amplitude modulator

The intensity is modulated, if the interaction is with a standing wave.

$$\begin{aligned}\Delta n(\mathbf{r},t) &= \Delta n \sin\omega_s t \cos(\mathbf{k}_s\mathbf{r}) = \frac{\Delta n}{4j}\{\exp[j(\omega_s t - \mathbf{k}_s\mathbf{r})] \\ &+ \exp[j(\omega_s t + \mathbf{k}_s\mathbf{r})] - \exp[-j(\omega_s t - \mathbf{k}_s\mathbf{r})] \\ &- \exp[-j\omega_s t + \mathbf{k}_s\mathbf{r}]\}\,.\end{aligned}$$

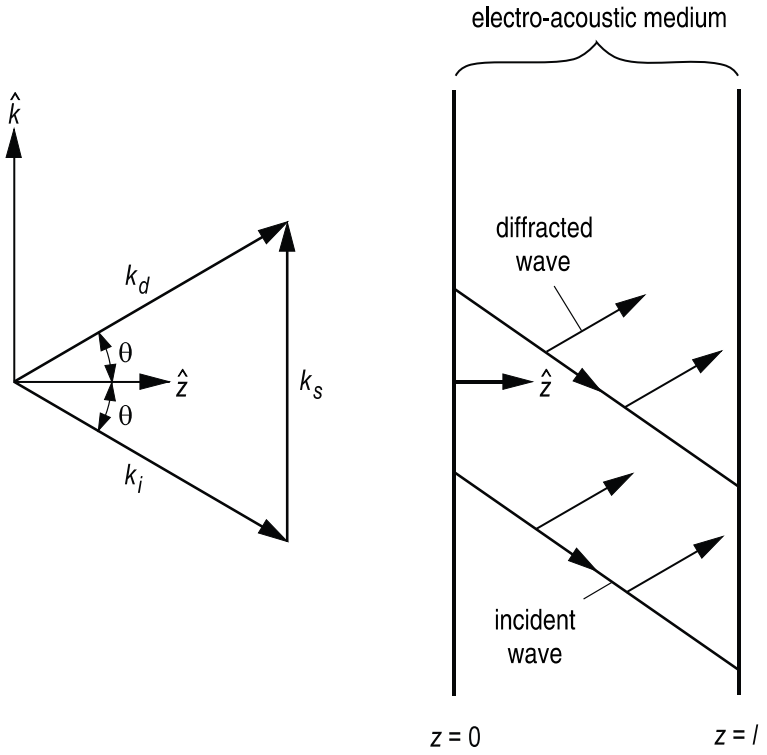

Figure 6.3: Momentum conservation in the acousto-optical amplitude modulator.

$$\omega_s << \omega_i \qquad \omega_d = \omega_i + m\omega_s$$

$$A_i(\ell) = A_i(0)\cos\left(\frac{\omega_i}{c}\frac{\Delta n}{2\cos\theta}\ell\right) \tag{6.20}$$

$$A_d(\ell) = -jA_i(0)\sin\left(\frac{\omega_i}{c}\frac{\Delta n}{2\cos\theta}\ell\right). \tag{6.21}$$

Afterwards the amplitude of the wave is simply made time-dependent, i.e., $\Delta n(t) = \Delta n \sin\omega_s t$. A graphical construction of both amplitudes is attempted in Fig. 6.4.

Again with the generating function of the Bessel functions, Eqs. (5.54) and (5.55),

$$\cos\left(x\sin\omega_s t\right) = \sum_{m\,\text{even}} J_m\left(x\right)e^{jm\omega_s t}, \tag{6.22}$$

$$\sin\left(x\sin\omega_s t\right) = -j\sum_{m\,\text{odd}} J_m\left(x\right)e^{jm\omega_s t}, \tag{6.23}$$

$$A_i(\ell) = A_i(0) \sum_{m\,\text{even}} J_m \left(\frac{\omega_i}{c} \frac{\Delta n}{2\cos\theta} \ell \right) e^{jm\omega_s t}, \tag{6.24}$$

$$A_d(\ell) = -A_i(0) \sum_{m\,\text{odd}} J_m \left(\frac{\omega_i}{c} \frac{\Delta n}{2\cos\theta} \ell \right) e^{jm\omega_s t}. \tag{6.25}$$

Two remarks need to be made. First, the incoming wave has only even sidebands and the diffractive wave only odd ones. I.e., the incoming wave is modulated with the frequency $2\omega_s$. The incoming wave is extinct, if the modulation depth is adjusted such that the Bessel function of zeroth order shows a zero or disappears, i.e., for

$$\frac{\omega_i}{c} \frac{\Delta n}{2\cos\theta} \ell = 2.405. \tag{6.26}$$

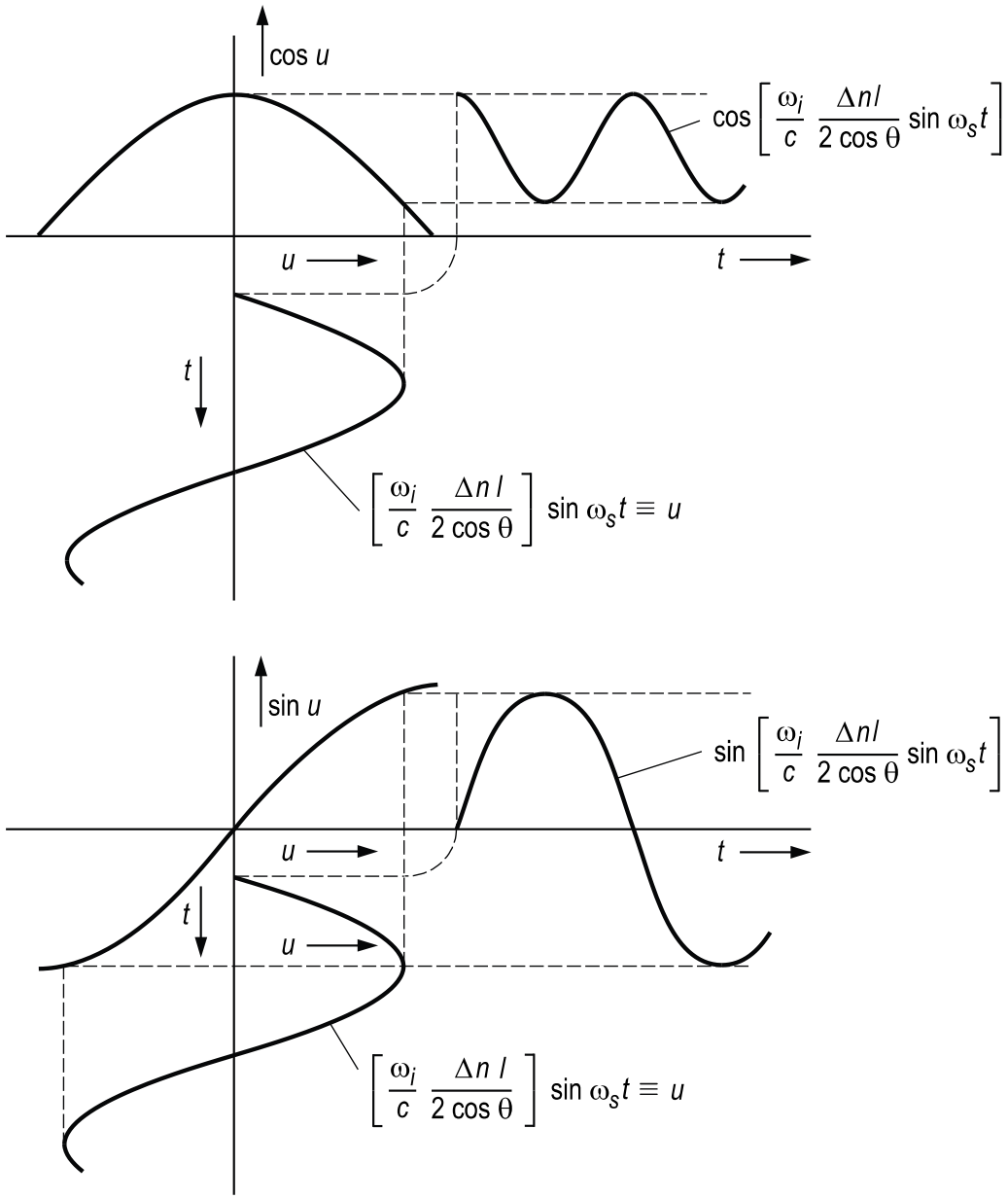

Figure 6.4: Time dependence of amplitudes for incoming and diffracted waves.

Chapter 7: Third-order nonlinear effects

third-harmonic generation (THG) or frequency tripling
self-phase modulation (SPM)

due to the possible different permutations of the input fields:

$$\chi^{(3)}(\omega:\omega,\omega,-\omega)=3\chi^{(3)}(3\omega:\omega,\omega,\omega)\frac{\chi^{(1)}(-\omega)}{\chi^{(1)}(3\omega)}, \qquad (7.1)$$

if no resonances in between the fundamental and third harmonic

7.1 Third-harmonic generation (THG)

THG possible in both centrosymmetric and non-centrosymmetric media,
also possible in solids and liquids
arguably the most interesting case: generation of UV and VUV in gases

$$\hat{P}^{(3)}(3\omega)=\frac{\varepsilon_0}{4}\chi^{(3)}(3\omega:\omega,\omega,\omega)\hat{E}(\omega)\hat{E}(\omega)\hat{E}(\omega). \qquad (7.2)$$

in low-conversion limit (almost always in THG), similar to SHG:

$$I(3\omega,\ell)=\left\{\frac{3\omega\chi^{(3)}(3\omega)}{8n_3c_0}\right\}^2\ell^2\left\{\frac{2}{n_1c_0\varepsilon_0}\right\}^2 I^3(\omega)\,\mathrm{sinc}^2\left\{\frac{\Delta k\ell}{2}\right\}. \qquad (7.3)$$

The conversion efficiency is given by

$$\frac{I(3\omega,\ell)}{I(\omega)} = \left\{\frac{3\omega\chi^{(3)}(3\omega)}{4n_3n_1c_0^2\varepsilon_0}\right\}^2 \ell^2 I^2(\omega)\,\mathrm{sinc}^2\left\{\frac{\Delta k\ell}{2}\right\}. \qquad (7.4)$$

For loosely focused Gaussian beams with a focal cross section $\left(\frac{\pi w_0^2}{2}\right)$ and confocal parameter $b \gg \ell$, we can write

$$\frac{P(3\omega,\ell)}{P(\omega)} = \frac{1}{3}\left\{\frac{3\omega\chi^{(3)}(3\omega)}{4c_0^2\varepsilon_0}\right\}^2 \frac{P^2(\omega)}{n_3n_1^3} \frac{\ell^2}{\left(\frac{\pi w_0^2}{2}\right)^2} \mathrm{sinc}^2\left\{\frac{\Delta k\ell}{2}\right\}. \qquad (7.5)$$

With stronger focusing, the Rayleigh range, over which the beam is focused, becomes smaller than the length of the conversion region

$$2b = \frac{2\pi w_0^2}{\lambda} \ll \ell$$

effective interaction length ~ Rayleigh range, i.e., $\ell_{eff} \sim 2b$

phase-matched case: $$\frac{P(3\omega)}{P(\omega)} \cong \frac{16}{3}\left\{\frac{3\omega\chi^{(3)}(3\omega)}{4c^3\varepsilon_0}\right\}^2 \frac{P^2(\omega)}{n_3n_1^3\lambda^2}. \qquad (7.6)$$

detailed calculation for case of strong focusing for third-order processes:

$$\ell_{eff} = 1.7b$$

G. C. Bjorklund, IEEE J. Quantum Electron. 11, 287 (1975)

in solids: in general difficult to achieve phase matching for THG
solution: SHG + subsequent SFG

in gases: by suitable mixing of different gases, the dispersion can be compensated, thus achieving phase matching,
THG conversion efficiencies up to 10% achieved

D. M. Bloom, G. W. Bekkers, J. F. Young, and S. E. Harris, Appl. Phys. Lett. **26**, 687 (1975).

7.2 The nonlinear refractive index

SPM effects come along with an additional factor 3 compared to THG, (due to number of possible permutations of input frequencies)
if only an electric field in *x*-direction:

$$\hat{P}_x^{(3)}(\omega) = \frac{3\varepsilon_0}{4}\chi_{xxxx}^{(3)}(\omega:\omega,\omega,-\omega)\left|\hat{E}_x(\omega)\right|^2\hat{E}_x(\omega) \qquad (7.8)$$

$$\hat{D}_x = \varepsilon_0\,\hat{E}_x + \hat{P}_x = \varepsilon_0\left\{1+\chi^{(1)}+\frac{3}{4}\chi^{(3)}\left|\hat{E}_x\right|^2\right\}\hat{E}_x \qquad (7.9)$$

$$= \varepsilon_0\, n^2\hat{E}_x \approx \varepsilon_0\left\{n_0^2+2n_0\Delta n\right\}\hat{E}_x, \qquad (7.10)$$

$$n = n_0 + \Delta n. \qquad (7.11)$$

$$\frac{3}{4}\chi^{(3)}\left|\hat{E}_x\right|^2 = 2n_0\Delta n$$

$$\Delta n = \frac{3}{8n_0}\chi^{(3)}\left|\hat{E}_x\right|^2.$$

linear polarization, definition via

electric field: $$\Delta n = \frac{1}{2}n_{2L}^{E}\left|\hat{E}_x\right|^2 \quad \rightarrow \quad n_{2L}^{E} = \frac{3}{4n_0}\chi^{(3)}, \tag{7.13}$$

intensity $$\Delta n = n_{2L}^{I} I_x \quad \rightarrow \quad n_{2L}^{I} = \frac{3}{4n_0^2 c_0 \varepsilon_0}\chi^{(3)}. \tag{7.14}$$

$$I_x = \tfrac{1}{2}n_0 c_0 \varepsilon_0 \left|\hat{E}_x\right|^2$$

A plane wave with arbitrary polarization in the x-y-plane is propagating in z-direction

$$\mathbf{E}(z,t) = \frac{1}{2}\left[\hat{E}_x(\omega)e^{j(\omega t - kz)} + c.c.\right]\hat{\mathbf{x}} + \frac{1}{2}\left[\hat{E}_y(\omega)e^{j(\omega t - kz)} + c.c.\right]\hat{\mathbf{y}} \tag{7.15}$$

in an instantaneously reacting, isotropic and lossless medium with third-order nonlinearity, thus it holds $\chi_{xxxx} = \chi_{xxyy} + \chi_{xyxy} + \chi_{xyyx}$. This gives rise to a nonlinear polarization (see problem set 2)

$$\hat{P}_x^{(3)}(\omega) = \frac{1}{4}\varepsilon_0 \chi_{xxxx}\left[3\left|\hat{E}_x\right|^2 \hat{E}_x + 2\left|\hat{E}_y\right|^2 \hat{E}_x + \hat{E}_y^2 \hat{E}_x^*\right] \tag{7.16}$$

$$\hat{P}_y^{(3)}(\omega) = \frac{1}{4}\varepsilon_0 \chi_{xxxx} \left[3 \left| \hat{E}_y \right|^2 \hat{E}_y + 2 \left| \hat{E}_x \right|^2 \hat{E}_y + \hat{E}_x^2 \hat{E}_y^* \right]. \qquad (7.17)$$

SPM XPM coherence term

description via circular polarizations

$$\hat{E}_\pm = \frac{1}{\sqrt{2}} \left(\hat{E}_x \pm j \hat{E}_y \right), \qquad (7.18)$$

$$\hat{P}_\pm^{(3)}(\omega) = \frac{1}{2}\varepsilon_0 \chi_{xxxx} \left[\left| \hat{E}_\pm \right|^2 \hat{E}_\pm + 2 \left| \hat{E}_\mp \right|^2 \hat{E}_\pm \right]. \qquad (7.19)$$

$$n_{2C} = \frac{2}{3} n_{2L}, \qquad (7.20)$$

independent, if the definition based on electric field or intensity

At first glimpse, it might be surprising that in the formulation in terms of circularly polarized light, see Eq. (7.19), no coherence term appears. However, this can be understood by the following argument: the difference phase between both polarizations enters the coherence term. This difference phase determines for equally strongly excited polarizations the orientation of the resulting superposed linear polarization. However, for linear polarization only self-phase modulation occurs and thus the polarization direction is conserved. If Eq. (7.19) contained a coherence term, this would result in a polarization-dependent polarization rotation, which, however, does not occur.

7.3 Molecular orientation and refractive index

A strong contribution to the nonlinear refractive index often stems from the orientation of an anisotropic molecule in an applied field. We therefore consider an ensemble of molecules, each of them possessing a linear polarizability $\alpha_{\parallel}$ in the direction of a distinguished axis of the molecule and a polarizability $\alpha_{\perp}$ perpendicular to that axis.

7.3.1 The Lorenz-Lorentz law

The dielectric displacement is given by

$$\mathbf{D} = \varepsilon_0 \mathbf{E} + \mathbf{P}, \tag{7.21}$$

where the polarization depends on the local field $\mathbf{E}_{local}$ via the molecules' density N and the average polarizability $\langle \alpha \rangle$ according to

$$\mathbf{P} = \varepsilon_0 N \langle \alpha \rangle \mathbf{E}_{local}. \tag{7.22}$$

The local field depends on the applied external field $\mathbf{E}$ and the resulting polarization $\mathbf{P}$ itself. To find the relation between the local field and external field and the polarization, we consider the microscopic spherical cavity inside a polarized isotropic medium shown in Fig. 7.1. The charge density on the surface of the sphere is given by $-P\cos\theta$, and the field at the center of the sphere due to this charge density is

$$\begin{aligned}\mathbf{E}_c &= \int_0^{\pi}\int_0^{2\pi} \frac{1}{4\pi\varepsilon_0 a^2}(\mathbf{P}\cos\theta)\cos\theta a^2\sin\theta d\theta d\phi \\ &= \int_0^{\pi} d\theta\cos^2\theta\sin\theta\frac{1}{2\varepsilon_0}\mathbf{P} = \frac{1}{3\varepsilon_0}\mathbf{P}. \qquad (7.23)\end{aligned}$$

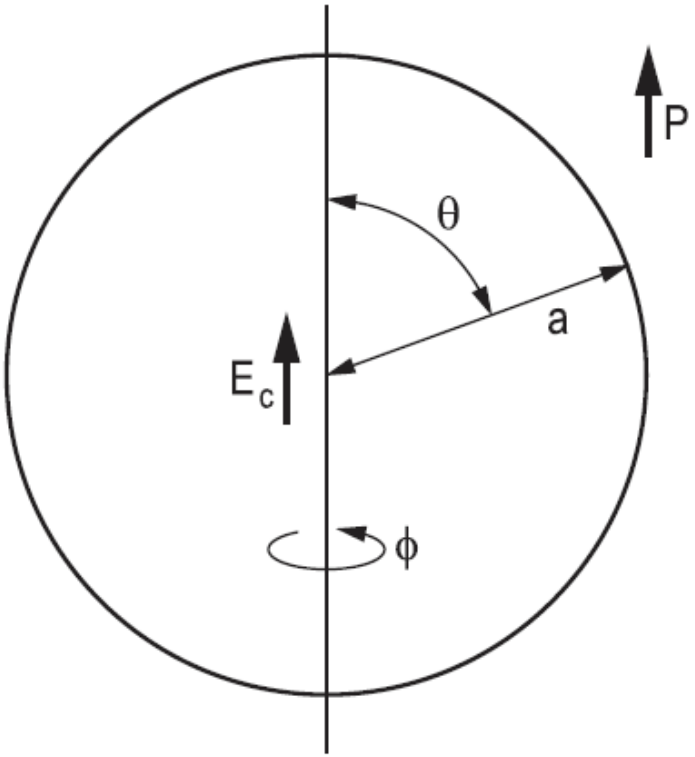

spherical cavity inside a polarized isotropic medium

The local field is the superposition of the external field and the field created by the polarization, i.e.,

$$\mathbf{E}_{local} = \mathbf{E} + \frac{1}{3\varepsilon_0}\mathbf{P}. \tag{7.24}$$

Using Eq. (7.22) we can eliminate the local field and it follows for the relation between the polarization and the externally applied field taking into account screening effects of the medium

$$\frac{\mathbf{P}}{\varepsilon_0 N \langle\alpha\rangle} = \mathbf{E} + \frac{1}{3\varepsilon_0}\mathbf{P}$$

or

$$\mathbf{P} = \varepsilon_0 \frac{N\langle\alpha\rangle}{1 - \frac{N\langle\alpha\rangle}{3}}\mathbf{E}. \tag{7.25}$$

The refractive index is defined via

$$\mathbf{P} = \varepsilon_0 (n^2 - 1)\mathbf{E}, \tag{7.26}$$

from which, by comparison with Eq. (7.25), we obtain the relation between average polarizability and refractive index

Clausius-Mossotti:

$$\frac{N\langle\alpha\rangle}{3} = \frac{n_0^2 - 1}{n_0^2 + 2}\,. \tag{7.27}$$

local field enhanced:

$$E_{local} = \left(\frac{n_0^2 + 2}{3}\right) E. \tag{7.28}$$

7.3.2 Intensity-dependent refractive index

If the axis of the molecule encloses an angle θ with the direction of the local field, then the polarization in the direction of the electric field is given by

$$P = N \left[\alpha_{\parallel} \left\langle \cos^2\theta \right\rangle + \alpha_{\perp} \left\langle \sin^2\theta \right\rangle\right] E_{local}$$

or according to Eq. (7.22)

$$\langle\alpha\rangle_0 = \left(\alpha_{\parallel} - \alpha_{\perp}\right) \left\langle \cos^2\theta \right\rangle + \alpha_{\perp}. \tag{7.29}$$

With

$$\left\langle \cos^2\theta \right\rangle = \frac{1}{4\pi} \int_0^{2\pi} \int_0^{\pi} \cos^2\theta \sin\theta d\theta d\phi = \frac{1}{3} \tag{7.30}$$

and Eq. (7.27), it then follows

$$\frac{n_0^2 - 1}{n_0^2 + 2} = \frac{N}{3} \langle\alpha\rangle = \frac{N}{9} \left\{\alpha_{\parallel} + 2\alpha_{\perp}\right\}. \tag{7.31}$$

canonical ensemble of molecules (temperature T)

exposed to external electric field

$$p(W) \sim \exp\left[-\frac{W}{k_B T}\right]$$

energy of dipole in electric field $W = -\frac{1}{2}\mathbf{P}\cdot\mathbf{E}_{local} = -\frac{1}{2}\alpha(\theta)\left|E_{local}\right|^2$

$$p(\theta) \sim \exp\left[-\frac{\left(\alpha_{\parallel}-\alpha_{\perp}\right)\left|E_{local}\right|^2\cos^2\theta}{2k_BT}\right].$$

Thus the field also changes the polarizability of the medium by partial orientation of the created dipoles. It holds

$$\left\langle\cos^2\theta\right\rangle = \frac{1}{2}\int_0^{\pi}\cos^2\theta p(\theta)\sin\theta d\theta \Big/ \frac{1}{2}\int_0^{\pi} p(\theta)\sin\theta d\theta$$

for small fields $\left\langle\cos^2\theta\right\rangle = \frac{1}{3}+\frac{4}{45}\frac{\left(\alpha_{\parallel}-\alpha_{\perp}\right)\left|E_{local}\right|^2}{2k_BT}.$

From the Lorenz-Lorentz relation (7.27), it then follows

$$\Delta\left\langle\alpha\right\rangle = \frac{4}{45}\frac{\left(\alpha_{\parallel}-\alpha_{\perp}\right)^2\left|E_{local}\right|^2}{2k_BT} = \frac{3}{N}\frac{6n_0\Delta n}{\left(n_0^2+2\right)^2}.$$

From this equation and the Lorenz-Lorentz relation (7.28) finally follows

$$n_2^E = \left(\frac{n_0^2+2}{3}\right)^2\frac{N}{45n_0}\frac{\left(\alpha_{\parallel}-\alpha_{\perp}\right)^2}{k_BT}. \qquad (7.32)$$

7.4 Self-phase modulation (SPM)

assume a purely linearly polarized or circularly polarized beam,

→ polarization is conserved

from Eq. (3.8) with $t' = t - z/v_g$ and $P_{NL} = 2\varepsilon_0 n \Delta n(E) E$

$$\frac{\partial}{\partial z} E(z,t') = -\frac{j\omega_0}{2nc_0\varepsilon_0} P_{NL} = -jk_0 \Delta n(E) E(z,t'), \qquad (7.33)$$

ansatz

$$E(z,t') = |E(z,t')|\, e^{-j\phi(z,t')} \qquad (7.34)$$

$$k_0 \Delta n(E) = \delta\, |E(z,t')|^2$$

SPM coefficient

$$\delta = k_0 n_{2L}^E / 2$$

$$\frac{\partial}{\partial z} |E(z,t')| - j\, |E(z,t')| \frac{\partial}{\partial z} \phi(z,t') = -j\delta\, |E(z,t')|^3$$

→

$$\frac{\partial}{\partial z} |E(z,t')| = 0$$

|envelope|^2 in time domain does NOT change

$$\frac{\partial}{\partial z} \phi(z,t') = \delta\, |E(z,t')|^2,$$

$$\phi(z,t') = \phi(0,t') + \delta\, |E(z,t')|^2 z.$$

phase modified ∝ instantaneous intensity

$$E(z,t) = e^{-j\delta |E(0,t)|^2 z} E(0,t). \qquad (7.36)$$

$$I(t) \sim |E(t)|^2$$

phase is only slowly varying in time,

instantaneous frequency

$$\Delta\omega(t) = -\frac{\partial\phi(t)}{\partial t} \quad (7.37)$$

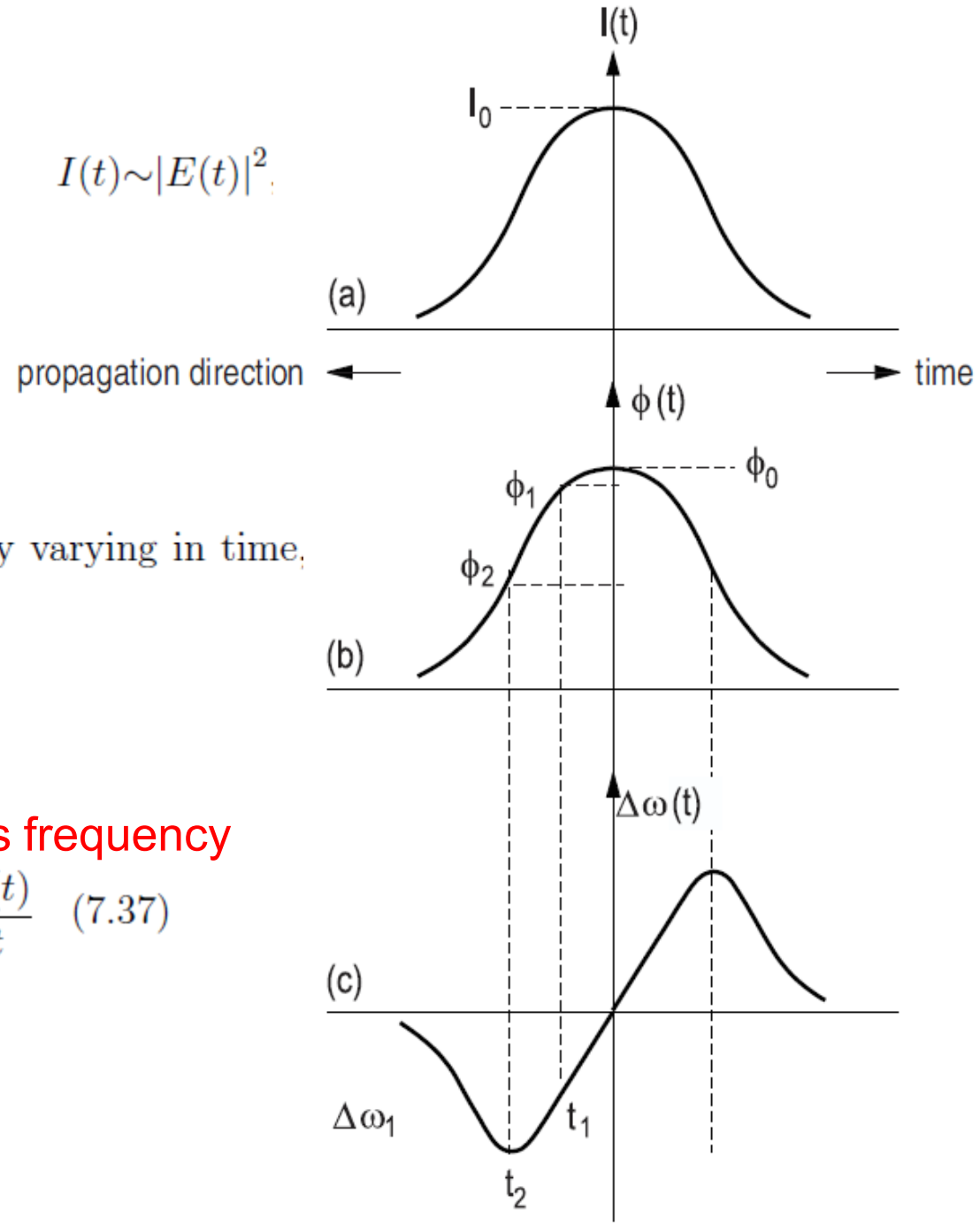

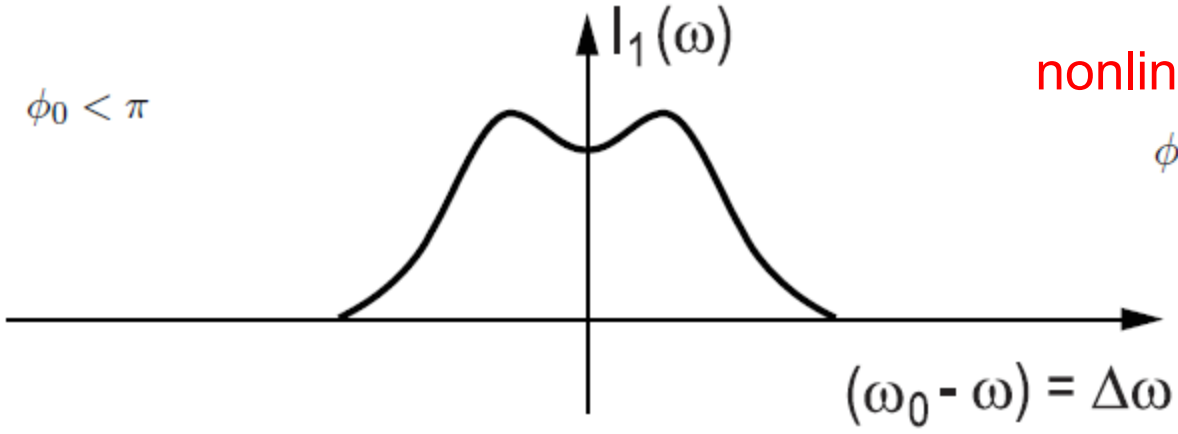

nonlinear phase shift

$$\phi_0 = \delta\,|E(0)|^2\,z.$$

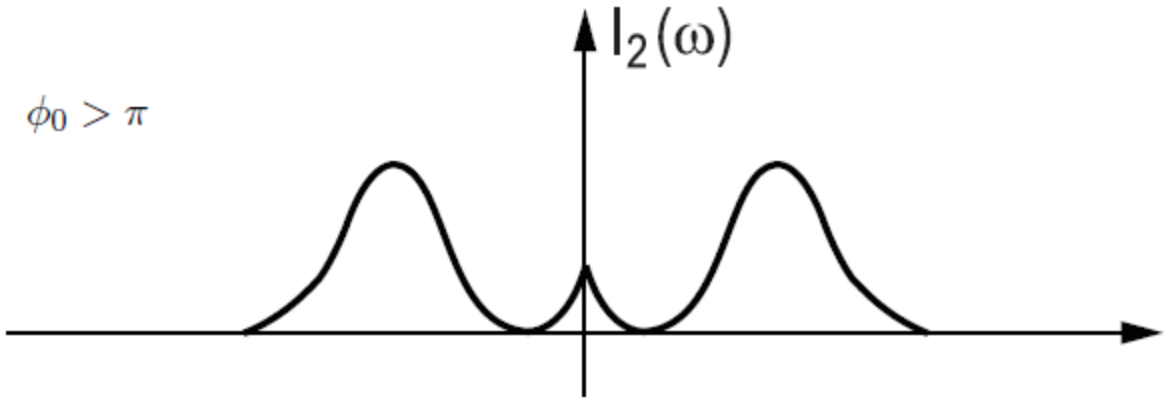

strong spectral broadening

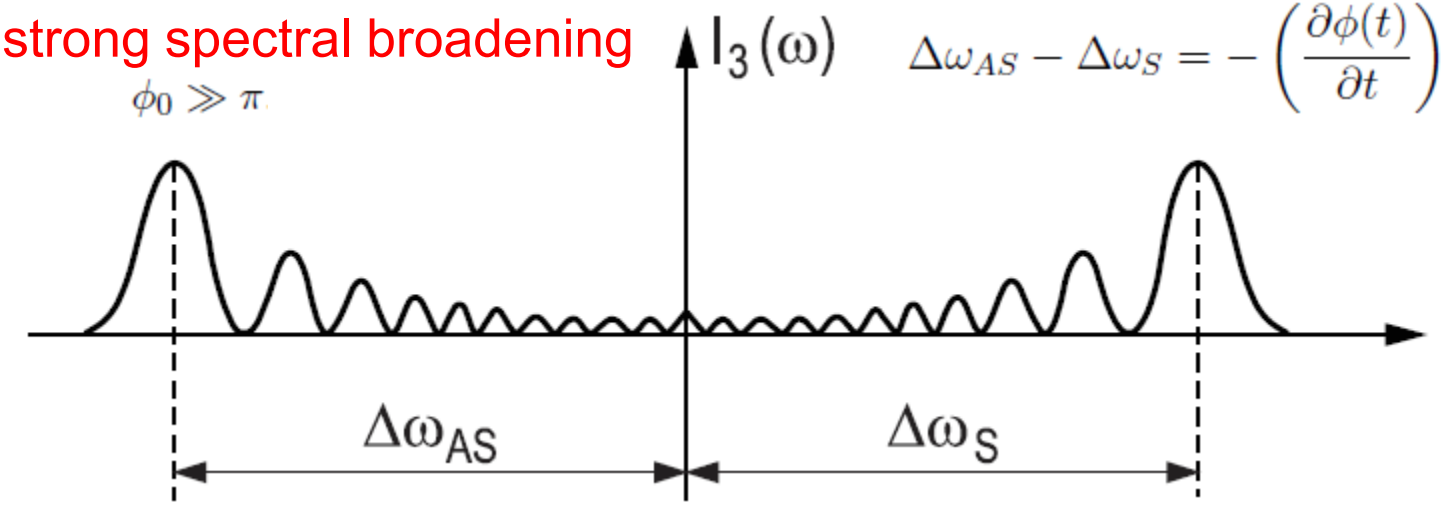

$$\Delta\omega_{AS} - \Delta\omega_S = -\left(\frac{\partial\phi(t)}{\partial t}\right)^R_{\max} + \left(\frac{\partial\phi(t)}{\partial t}\right)^F_{\max} \qquad (7.38)$$

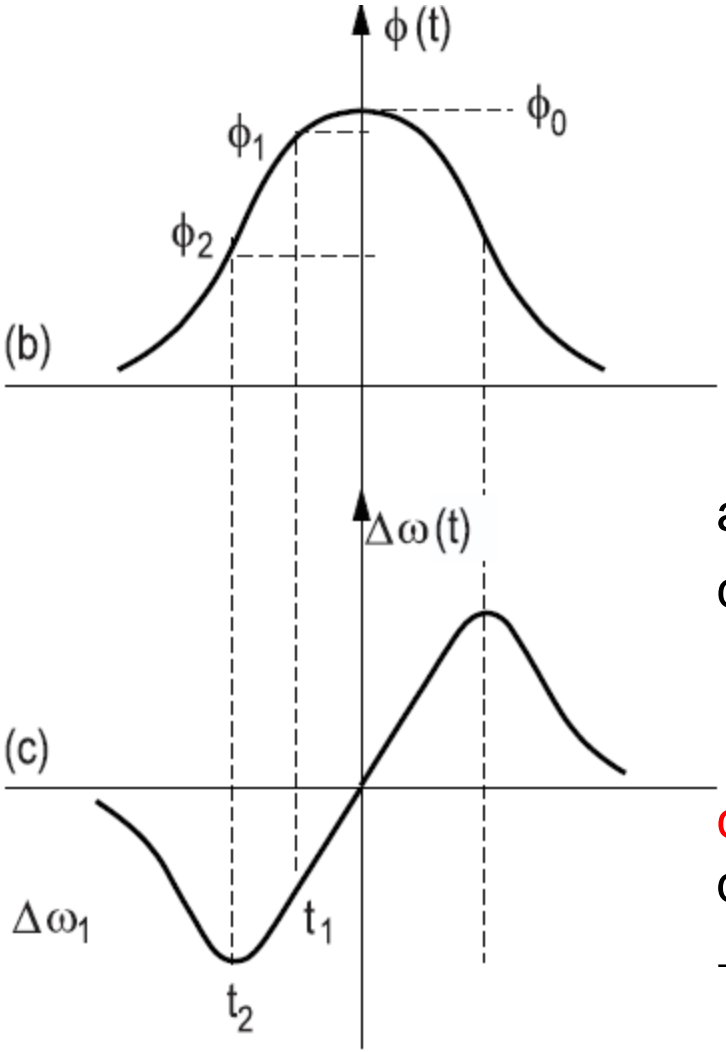

always two instants during the pulse, which contribute to the same generated frequency

constructive/destructive interference depending on relative phase at these times

→ maxima/minima in SPM spectrum

zero points in spectrum for $\phi_0 = (2m+1)\,\pi$

number of minima N on one side of the spectrum: $(2N+1) \geq \frac{\phi_0}{\pi} \geq (2N-1)$

SPM for Gaussian pulse: $I(t) = I_0 \exp\left[-\frac{t^2}{\tau^2}\right]$ (7.41)

$$\begin{aligned}
\phi(t) &= \phi_0 \exp\left[-\frac{t^2}{\tau^2}\right] \\
\Delta\omega_{AS} - \Delta\omega_S &= 2\left|\left(\frac{\partial\phi(t)}{\partial t}\right)\right|_{\max} \\
&= 4\phi_0 \left|\frac{t}{\tau^2}\exp\left[-\frac{t^2}{\tau^2}\right]\right|_{\max}, \rightarrow \frac{t}{\tau} = \frac{1}{\sqrt{2}} \\
&= 2\sqrt{\frac{2}{e}}\frac{\phi_0}{\tau} \approx 1.71\frac{\phi_0}{\tau}. \qquad (7.42)
\end{aligned}$$

From the relations for the full width at half maximum (FWHM)

$$\tau = \frac{\tau_{FWHM}}{1.665} \qquad (7.43)$$

and the time-bandwidth product of a Gaussian pulse

$$\Delta\omega_{FWHM} = \frac{0.44}{\tau_{FWHM}} 2\pi, \qquad (7.44)$$

we obtain for the spectral broadening of a Gaussian pulse

$$\frac{\Delta\omega_{AS} - \Delta\omega_S}{\Delta\omega_{FWHM}} = \frac{1.71 \cdot 1.665}{0.44 \cdot 2\pi}\,\phi_0 = 1.03\,\phi_0. \qquad (7.45)$$

7.5 Self-focusing

transverse beam profile becomes instable

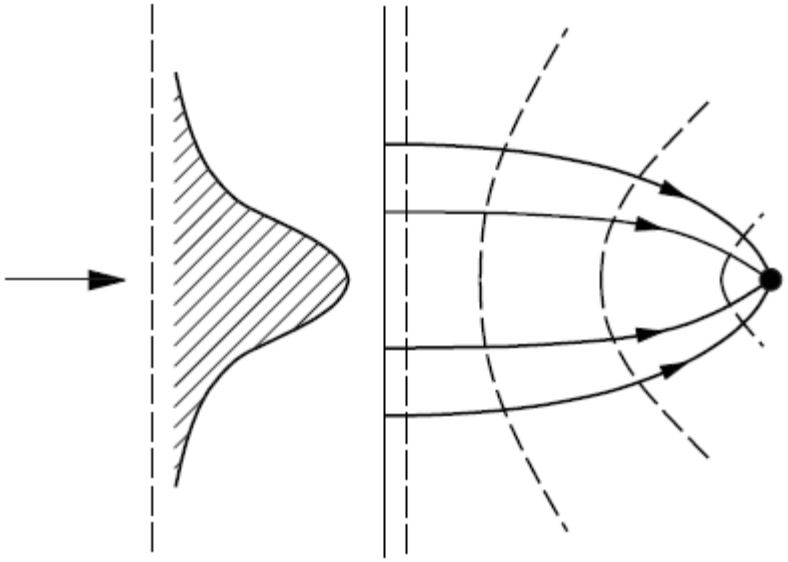

intensity-dependent refractive index

for $\Delta n_2 > 0$:

- phase velocity in center reduced
- phase fronts bend due to the induced lens (”**Kerr lens**”)
- self-focusing of the beam

R. Y. Chiao, E. Garmire, and C. H. Townes, Phys. Rev. Lett. **13**, 479 (1964).

H. A. Haus, Appl. Phys. Lett. **8**, 128 (1966).

relevance:

- Kerr-lens mode-locked laser oscillators
- unwanted detrimental effect of ”hot spots”

simple physical consideration in 2D:

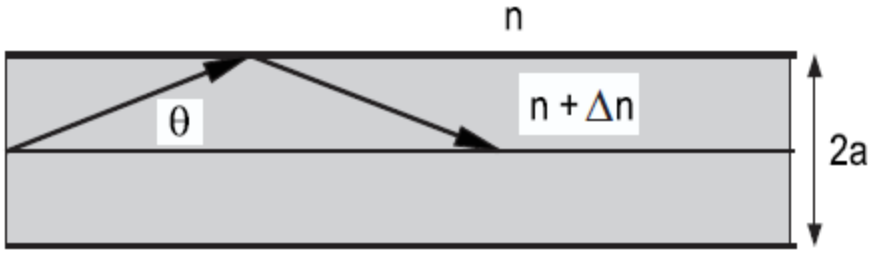

Snell's law → total internal reflection for $\theta < \theta_c$, with $\cos\theta_c = \frac{n}{n+\Delta n}$

$$\cos\theta_c \cong 1 - \frac{\theta_c^2}{2} \cong 1 - \frac{\Delta n}{n} \Rightarrow \theta_c \cong \sqrt{2\Delta n/n}. \tag{7.46}$$

If a beam of diameter $2a$ propagates through the medium, it contains, because of diffraction, rays with an angle

$$\theta_B = \left(\frac{\pi/a}{k_0 n}\right) = \frac{\lambda/n}{2a}. \tag{7.47}$$

The refractive index difference, for which all these rays are totally reflected (i.e., trapped) then follows from $\theta_c = \theta_B$, thus

$$\Delta n_c = n_2^I I_c = \frac{\theta_c^2}{2} n. \tag{7.48}$$

From this we obtain, independent of the beam diameter, a critical power of the beam

$$P_c = \frac{\pi\lambda^2}{8nn_2}. \tag{7.49}$$

$$P_c = \frac{\pi \lambda^2}{8 n n_2}. \qquad (7.49)$$

above this critical power, self-focusing exceeds diffraction.

Note the **quadratic scaling with wavelength**!

in 2D (1 longitudinal, 1 transversal dimension): **spatial solitons** occur.

in 3D (2 transversal dimensions):
catastrophic self-focusing occurs, that eventually is balanced by other nonlinear effects, e.g.,
- saturation of the intensity-dependent refractive index
- self-defocusing due to plasma formation by multi-photon ionization (**"filamentation"**)

A. Couairon and A. Mysyrowicz, Phys. Reports **441**, 47 (2007).

L. Bergé, S. Skupin, R. Nuter, J. Kasparian, and J.-P. Wolf, Rep. Prog. Phys. **70**, 1633 (2007).

In the paraxial approximation

$$k_z = \sqrt{k^2 - \left(k_x^2 + k_y^2\right)} \approx k - \frac{1}{2k}\left(k_x^2 + k_y^2\right). \tag{7.50}$$

The dispersion relation within the paraxial approximation reads

$$\frac{\omega}{c} - k_z - \frac{1}{2k}\left(k_x^2 + k_y^2\right) = 0. \tag{7.51}$$

Taylor expansion around the carrier wave with carrier frequency and wave number in z-direction (ω_0, k_0), i.e., $\omega = \omega_0 + \Delta\omega$ and $\mathbf{k} = (\Delta k_x, \Delta k_y, k_0 + \Delta k_z)$, yields

$$\frac{\Delta\omega}{v_g} - \Delta k_z - \frac{1}{2k_0}\left(\Delta k_x^2 + \Delta k_y^2\right) = 0. \tag{7.52}$$

For the envelope $E(x, y, z, t)$ of a linearly polarized pulse propagating in positive z-direction

$$E(x, y, z, t) = \int\int\int d^3\left(\Delta k\right) E(\Delta k_x, \Delta k_y, \Delta k_z) e^{j(\Delta\omega t - \mathbf{\Delta k x})} \tag{7.53}$$

allowing for the nonlinear polarization (from Chapter 3), we obtain

$$\frac{1}{v_g}\frac{\partial E}{\partial t} + \frac{\partial E}{\partial z} + \frac{j}{2k_0}\nabla_\perp^2 E = -jk_0\Delta n E. \tag{7.54}$$

In cylindrical coordinates and with the ansatz

$$E(r,z,t) = E_0(r,z,t)\exp\{-j\phi(r,z,t)\}$$

we arrive at the following two equations

$$\left[\frac{1}{v_g}\frac{\partial\phi}{\partial t}+\frac{\partial\phi}{\partial z}\right]+\frac{1}{2k_0}\left[\frac{\partial\phi}{\partial r}\right]^2 = \underbrace{k_0\Delta n}+\underbrace{\frac{1}{2k_0E_0}\left[\frac{\partial^2E_0}{\partial r^2}+\frac{1}{r}\frac{\partial E_0}{\partial r}\right]} \quad (7.55)$$

$$= \text{self-focusing} + \text{diffraction}$$

$$\left[\frac{1}{v_g}\frac{\partial E_0}{\partial t}+\frac{\partial E_0}{\partial z}\right]+\frac{1}{k_0}\frac{\partial\phi}{\partial r}\frac{\partial E_0}{\partial r}+\frac{1}{2k_0}E_0\left[\frac{\partial^2\phi}{\partial r^2}+\frac{1}{r}\frac{\partial\phi}{\partial r}\right]=0. \quad (7.56)$$

If a stationary beam exists, for which self-focusing and diffraction exactly balance each other during propagation, then it must hold $\frac{\partial E_0}{\partial t}=\frac{\partial E_0}{\partial z}=0$, from which in combination with Eq. (7.56) follows

$$\frac{\partial\phi}{\partial r}=0.$$

I.e., this solution exhibits a plane phase front. Eq. (7.55) then simplifies to

$$-n_2^E E_0^2 = \frac{1}{k_0^2E_0}\left[\frac{\partial^2E_0}{\partial r^2}+\frac{1}{r}\frac{\partial E_0}{\partial r}\right]. \quad (7.57)$$

This equation was solved numerically [3, 4]. The stationary solution with the lowest critical power yields

$$P_c = \left(\frac{5.763}{4\pi^2}\right)\frac{\varepsilon_0 c_0 \lambda^2}{n_2^E} = \left(\frac{5.763}{4\pi^2}\right)\frac{\lambda^2}{n n_2^I} \approx \frac{1}{7}\frac{\lambda^2}{n n_2^I}. \tag{7.58}$$

This is of the same order of magnitude as the simple estimate of Eq. (7.49). However, Eq. (7.57) permits to gain deeper insights into the process of self-focusing. It can easily be shown by insertion into Eq. (7.57) that, if $E_0(r)$ is a solution of Eq. (7.57), then also the scaled function $\gamma^2 E_0(\gamma r)$ is a solution. All these solutions contain the same guided energy

$$\int_{-\infty}^{\infty} \gamma^2 E_0^2(\gamma r)\, r dr = \int_{-\infty}^{\infty} E_0^2(r')\, r' dr'$$

$$P = \frac{n_{eff}}{2}\sqrt{\varepsilon_0/\mu_0}\int_{-\infty}^{\infty} E_0^2(r)\, r dr.$$

This scaling invariance is one of the few exact results of self-focusing theory, which reveals that the beam is not stable in 3D. This changes if only one transverse dimension exists, the other dimension could be fixed, e.g., using a waveguide, then it holds according to Eq. (7.54)

$$\frac{1}{v_g}\frac{\partial E}{\partial t} + \frac{\partial E}{\partial z} = -j\frac{1}{2k_0}\frac{\partial^2}{\partial x^2}E - jk_0 n_2^E |E|^2 E. \tag{7.59}$$

Introducing the retarded time $t' = t - z/v_g$, it follows

$$\frac{\partial E(t',z)}{\partial z} = -j\frac{1}{2k_0}\frac{\partial^2}{\partial x^2}E - jk_0 n_2^E \left|E\right|^2 E. \tag{7.60}$$

Again it is straightforward to show by insertion, that this equation, which is called nonlinear Schrödinger equation, possesses solutions

$$E(t',z) = E_0 \mathrm{sech}\left[\frac{x}{x_s}\right] e^{-jk_s z}, \tag{7.61}$$

if the following relations are fulfilled

$$k_s = \frac{1}{2}k_0\frac{n_2^E}{2n}\left|E_0\right|^2, \quad k_s = \frac{1}{2k_0 x_s^2}. \tag{7.62}$$

For a given power density guided in y-direction, that is proportional to

$$\int_{-\infty}^{\infty} E_0^2(x)\,dx = 2\left|E_0\right|^2 x_s,$$

there is now only one solution, because the different solutions of form $\gamma^2 E_0^2(\gamma x)$ belong to different power densities. We will later discuss the properties of the nonlinear Schrödinger equation in greater detail, here we already point out that the solutions (7.61) correspond to a spatial soliton.

For powers far above the critical power for self-focusing, the beam with a Gaussian input profile is focusing down within a distance z_f This distance can be estimated as follows employing a parabolic approximation. The parabolic intensity distribution in the Gaussian beam, $I(r) = I_0 \exp[-r^2/w_0^2]$, induces in the center of the beam a lens, which bends the phase fronts of the beam

$$\Delta\phi(r) = k_0 n_2^I (I(r) - I_0) z \approx -k_0 n_2^I I_0 \frac{r^2}{w_0^2} z.$$

This phase shift corresponds to the effect of a lens or a spherical focusing mirror with radius R according to

$$\Delta\phi(r) = -k_0 \frac{r^2}{2R}.$$

As the beam is focusing within a distance $z = z_f \approx R$, it thus follows

$$k_0 n_2^I I_0 \frac{r^2}{w_0^2} z_f = k_0 \frac{r^2}{2z_f}$$

and therefore

$$z_f = \frac{w_0}{\sqrt{2n_2^I I_0}}. \qquad (7.63)$$

With the critical power for self-focusing according to Eq. (7.58), we obtain

$$z_f = 0.52 k_0 w_0^2 \sqrt{\frac{P_c}{P}} \approx b \sqrt{\frac{P_c}{P}}. \tag{7.64}$$

Numerical simulations yield

$$z_f = 0.71 b \left(\sqrt{\frac{P}{P_c}} - 0.86 \right)^{-1}. \tag{7.65}$$

As an example, we consider self-focusing in sapphire. At 800-nm wavelength, sapphire has a linear refractive index of about $n = 1.8$ and an intensity-dependent refractive index coefficient of $n_2^I = 3 \times 10^{-16}$ cm^2/W. With this we obtain from Eq. (7.58) a critical power for self-focusing of $P_c = 2.7$ MW.

Photograph of a self-guided filament induced in air by a high-power infrared (800 nm) laser pulse [from http://www.teramobile.org]

Remote detection of biological aerosols. The tube in the center of the picture is an open cloud chamber generating the bioaerosol simulant. The laser beam is arriving from the left. [from http://www.teramobile.org]

High-voltage lightning: (left) without laser guiding, (right) with laser guiding.
[from http://www.teramobile.org]